AabZIP1 confers drought tolerance and promotes artemisinin biosynthesis in Artemisia annua

guoping Shu¹, yueli Tang¹, mingyuan Yuan¹, chunxue Jiang¹, Wanhong Liu², Fangyuan Zhang¹, Chunxian Yang¹, Xiaozhong Lan³, Min Chen¹, lien Xiang⁴, and Zhihua Liao¹

¹Southwest University ²Chongqing University of Science and Technology ³Xizang Agricultural and Husbandry College ⁴China West Normal University

March 30, 2022

Abstract

Water deficiency is one of the most major factors that limit plant growth and agricultural productivity. Previous studies showed the biomass and artemisinin content reduced significantly in A. annua plant under water scarcity. However, the molecular mechanism by which A. annua responds to drought stress is not well understood. In this study, AabZIP1 was identified to be involved in the responsive process to drought stress in A. annua. AabZIP1 could activate the expression of two wax biosynthesis genes, AaCER1 and AaCYP86A1, by directly binding to their promoters. Overexpression of AabZIP1 significantly promoted the expression of AaCER1 and AaCYP86A1 and led to enhanced cuticular waxes biosynthesis, thus significantly elevating the tolerance to water deficiency in A annua. Additionally, AabZIP1 positively regulates the expression of AaMYC2 by binding to its promoter, a MYC family transcription factor which positively regulates the expression of artemisinin biosynthesis genes, like ALDH1, DBR2 and CYP71AV1. Overexpression of AabZIP1 caused the upregulation of the expression of AaMYC2 and artemisinin biosynthesis genes, leading to an increase of artemisinin content. Taken together, our results indicate that AabZIP1 plays a positive role in the regulation of drought tolerance and artemisinin biosynthesis in A annua.

Introduction

Artemisia annua , a traditional Chinese medicinal plant, is well-known for producing anti-malarial artemisinin. Apart from its irreplaceable function for malaria treatment, artemisinin also shows great potential in the treatment of lupus erythematosus (Tu, 2011), diabetes (Li et al., 2017), tuberculosis (Miller et al., 2011) and malignant tumors (Tran et al., 2014). With the discovery of new uses of artemisinin, the demand for the chemical is growing worldwide. Artemisinin can be synthesized chemically, and its synthetic precursors have also been successfully obtained in *Escherichia coli* and *Saccharomyces cerevisiae* through recombinant microbial pathways (Anthony et al., 2009; Westfall et al., 2012), which can realize semi-synthetic production of artemisinin. Unfortunately, these methods are difficult to use for poor Southeast Asian and African countries due to their high cost, and therefore can't be used as the staple method for production of artemisinin now and for a long time in the future (Graham et al., 2010). So it is quite important to develop the A. annua germplasm resources with high artemisinin content and strong tolerance to environmental stress.

Drought is one of the main environmental factors affecting plant growth and crop yield (Lesk, Rowhani, & Ramankutty, 2016; Li et al., 2019). Water deficiency causes dramatic changes in physiological and biochemical processes in plants (Anjum et al., 2011). An increasing number of studies revealed that the metabolism and productivity were decreased in wheat (Tabassum et al., 2017), rice (Selvaraj et al., 2017)

and maize (AbdElgawad et al., 2020) under water deficiency for a long period of time. For *A. annua*, previous research revealed that drought stress caused a decline in the levels of many metabolites (including artemisinin) and biomass, and water deficit induced a decrease in glandular trichome (secrete and store artemisinin) density and size as well (Yadav et al., 2014; Vashisth et al., 2018). To cope with drought stress, plants have evolved many sophisticated adaptive mechanisms regulating physiological and cellular level traits to relieve the stress (Obata et al., 2012; Li et al., 2019), such as increasing the accumulation of cuticular wax.

Plant organs are covered with a layer of cuticular wax, which acts as a protective barrier to prevent excessive water loss across the primary surface under water deficit (Seo and Park, 2011; Li et al., 2019; Dimopoulos et al., 2020). Cuticular waxes are mainly composed of a series of very long-chain aliphatic compounds, including acyl esters (wax esters), alkanes, aldehydes, fatty acids, primary alcohols, secondary alcohols and ketones (Kunst et al., 2003; Lee and Suh, 2013). The internal regulatory mechanism controlling these cuticular waxes biosynthesis is relatively complex. At present, more than 190 genes have been reported to be involved in wax biosynthesis in Arabidopsis. For example, CER1 is the sole enzyme required for alkane-forming, which has been identified from various plant species such as Arabidopsis and rice (Jung et al., 2006; Bernard et al., 2012). It has recently been reported that TaCER1 is involved in cuticular wax alkane formation and is likely involved in the response to drought stress (Li et al., 2019). Moreover, ArabidopsisCYP86A1 gene was found to catalyze the ω -hydroxylation of saturated and unsaturated fatty acids with chain lengths from C12 to C18, and also suggested to be involved in suberin formation as a protective layer (Höfer et al., 2008). Many studies have shown that the expression of genes involved in wax biosynthesis is significantly increased under drought stress (Aharoni et al., 2004; Zhang et al., 2005; Seo and Park, 2011). The upregulation of these genes under drought stress is caused by the activation of stress-induced transcription factors (TFs) in plants (Howell, 2013), such as SIMYB31, which promotes cuticular wax biosynthesis in response to drought stress (Xiong et al., 2020). In A. annua, several transcription factors, such as AaMIXTA1 and AaHD8, were reported to positively regulate the expression of wax biosynthesis genes, including CER1, CYP86A1 ,KCS5 and FDH, etc. (Shi et al., 2017; Yan et al., 2018). However, up to now, there is little known about the molecular link between drought stress and cuticular waxes biosynthesis in A. annua.

Previous research showed that drought treatment could induce the transcription of AabZIP1, an ABAinduced bZIP transcription factor in A. annua (Zhang et al., 2015). Besides, bZIP transcription factors were reported to play an important role in response to abiotic stress such as drought (Que et al., 2015). So it is quite interesting to explore the definite roles of AabZIP1 in drought response in A. annua.

Moreover, it was found that AabZIP1 directly activates the transcription of two artemisinin biosynthesis genes, ADS and CYP71AV1 (Figure S1), by binding to their promoters and promotes artemisinin biosynthesis in *A. annua* (Zhang et al., 2015). But it's not known whether AabZIP1 can regulate the transcription of DBR2 and ALDH1, another two genes involved in artemisinin biosynthesis. Recently, AaMYC2 and AaGSW1, whose expression is induced by MeJA and ABA, have been reported to positively regulate artemisinin biosynthesis (Shen et al., 2016; Chen et al., 2017). Among them, AaGSW1 directly activates the transcription of CYP71AV1, and AaMYC2 directly activates the transcription of CYP71AV1, and DBR2 respectively. Interestingly, AabZIP1 and AaMYC2 both directly regulate the transcription of AaGSW1, and they form a feed-forward loop in the regulation of artemisinin biosynthesis (Chen et al., 2017). These results indicate that TFs involved in phytohormone signaling form a relatively complex regulatory network in artemisinin biosynthesis. Therefore, it is worthwhile to further dissect the regulatory mode by which AabZIP1 regulates artemisinin biosynthesis.

In this study, we found that the AabZIP1-overexpressing A. annuaplnats exhibited higher drought tolerance, and investigated the molecular mechanism underlying such drought tolerance. It is revealed that AabZIP1 directly activates the expression of two wax biosynthesis genes through binding to the ABRE *cis* -elements in their promoters, thus promoting cuticular wax accumulation and leading to higher resistance to water deficiency. These results indicate AabZIP1 plays a positive role in regulating cuticular wax biosynthesis and participating in drought stress response. In addition, we found AabZIP1 can activate the expression of *DBR2*

and ALDH1 via an indirect AaMYC2-dependent pathway to promote artemisinin production. Our findings revealed the positive roles of AabZIP1 in regulating drought tolerance and artemisinin biosynthesis in A. *annua*, and expand the knowledge for the regulatory network in artemisinin biosynthesis and response to environmental stress.

Materials and Methods

Plant cultivation and water drought treatment

Seeds were harvested from wild-type A. annua grown in the experimental field of Southwest University (Chongqing, China) for this study. These seeds were surface-sterilized with 15% sodium hypochlorite solution for 20 min, and then washed three times with sterile water. Subsequently, seeds were germinated on 1/2 MS solid medium at $23 \pm 2^{\circ}$ C under a light period of 16-h light /8-h dark. All seedlings were grown in pots with organic substrates in an artificial climate room at $23 \pm 2^{\circ}$ C under a light period of 16-h light/8-h dark. All seedlings were grown in pots with organic substrates in an artificial climate room at $23 \pm 2^{\circ}$ C under a light period of 16-h light/8-h dark \circ Nicotiana benthamiana seeds were sown directly in soil and their growth conditions are consistent with that of A. annua plants. Tobacco plants grown for 6 weeks old were used for dual-luciferase assays. For drought stress, when the soil where the A. annua plants grow shows signs of slight water deficiency, it is regarded as the initiation of drought stress. After 8 days of drought stress, re-water the plants to provide normal growth conditions. In addition, A. annua plants for 5 weeks old at 0, 3, 6, 12 and 24 h after drought stress and well-water conditions were collected for genes expression analysis.

Artemisia annua plant transformation

For obtaining the reconstruction plasmid of pHB-AabZIP1, AabZIP1 was inserted into pHB plasmid driven by double CaMV 35S promoter through BamH1 and Pst1 sites, and then transferred into A. tumefaciensstrain EHA105 to form engineering strains. These strains were grown on YEP solid medium containing related antibiotics for 48 h. Subsequently, positive monoclonal strain was inoculated into YEP liquid medium containing related antibiotics for culture until the OD600 value of the medium reaches 0.6. The supernatant was discarded after centrifugation, and then resuspended in the 1/2 MS liquid to OD600 = $0.3^{\circ}0.5$, 200 rpm shaking culture at 28°C for 30 min. Cultured engineered strains were used to transform A. annua viaAgrobacterium -mediated transformation as described previously (Shen et al., 2012). After that, the obtained seedlings were transplanted into pots with organic substrates and cultured in an artificial climate room at $23 \pm 2^{\circ}$ C under a light period of 16-h light /8-h dark.

Quantitative real-time PCR

The 5 weeks old wild-type A. annua were treated with water deficiency. All leaves of A. annua plants at 0, 3, 6, 12 and 24 h after drought stress and well-water conditions were collected and then frozen immediately in liquid nitrogen. Similarly, 5 weeks old wild-type A. annua were treatment with 10 μ M exogenous ABA in 0.5% ethanol, while 0.5% ethanol as the mock treatment. All leaves of A. annua plants at 0, 3, 6, 12 and 24 h after exogenous ABA and mock treatment were collected, and then frozen immediately in liquid nitrogen. The total RNA of these samples was extracted using the total plant RNA Extract Kit (Tiangen, China), and then reversely transcribed into cDNA using FastKing RT Kit (with DNase) FastKing cDNA (Tiangen, China). Subsequently, the cDNA was used as the template to detect the expression levels of AabZIP1 and wax biosynthesis genes by quantitative real-time PCR (qRT-PCR) experiment. The qRT-PCR amplification conditions were 95°C for 3 min, followed by 40 cycles of 95°C for 10 s, 56°C for 20 s, and 72°C for 20 s. The β -actin of A. annua was used as the reference gene in this study (Wang et al., 2009). The relative expression levels of target genes were calculated using the 2^{-T} method (Livak and Schmittgen, 2001). The primer sequences in qRT-PCR were listed in Supplementary Table S1.

Scanning electron microscopy (SEM)

In order to observe the accumulation of cuticular waxes, scanning electron microscopy (SEM) was carried out using methods reported previously (Shi et al., 2017). The fifth leaf of 5 weeks old AabZIP1-overexpression transgenic and wild-type *A. annua* were fixed in 2.5% Glutaraldehyde fixative at room temperature for 5 h, respectively. The fixed leaves were washed three times with 0.1 M phosphate buffer (pH 7.0) for 10 min

each time, dehydrated for 10 min through a series of alcohol concentration gradient (30%, 40%, 50%, 60%, 70%, 80%, 95%), and then samples were dehydrated three times with 100% ethanol for 5 min each time and dried in a critical point drying device (Leica 011206, Germany). The prepared samples were coated with 20 A gold particles, and the observation of cuticular waxes were fulfilled by SEM (Phenom-World BV, Phenom Pro010102).

Plant leaf cuticular waxes extraction and GC-MS analysis

For cuticular waxes analyses, a total of 0.5g fresh leaves from AabZIP1-overexpression transgenic and wildtype A. annua were collected and thoroughly extracted with 5 ml chloroform for 3 min at room temperature. The supernatant was filtered through a 0.22 μ m-size filters and then the solvents were lyophilized through a gentle stream of nitrogen. The resulting residues were dissolved with 500 μ l chloroform, and then these mixtures were transferred into 1.5 ml tube and dried again under a gentle stream of nitrogen. The resulting residues was derivatized with a mixture of 100 μ l pyridine and 100 μ l bis-N, N- (trimethylsilyl) trifluoroacetamide for 1 h at 70°C and then 1000 μ l n-heptane containing tricosane (as internal standard) was added to dilute the solution. The solution was centrifuged at 12000 rpm for 5 min. The supernatant was analyzed by gas chromatography-mass spectrometry (GC-MS-QP2010 Ultra; Shimadzu) with the temperature program: initial temperature of 70 (1 min hold), increase to 160 at 10/min, and then ramp to 240 at 5/min. Finally, increase to 280 at 20/min (17 min hold). Helium was used as a carrier gas and 1 μ l sample was injected in split mode; split rate, 2:1; ion source temperature, 230; ionization voltage, 70 eV with scanning from m/z 33 to 500. Qualitative analysis of all compounds was fulfilled by comparing with NIST (National Institute of Standards and Technology) database and Wiley libraries. The relative content of all compounds was calculated by comparing peak areas with that of the internal standards.

Measurement of artemisinin and dihydroartemisic acid

For artemisinin and dihydroartemisic acid analyses, mature leaves of 16 weeks old AabZIP1-overexpression and wild-type *A. annua* plants were collected and drying at 50 °C, and then used for the detection of artemisinin and dihydroartemisic acid contents using HPLC as described previously (Xiang et al., 2019). At least three replications were completed. Standard samples of artemisinin and dihydroartemisic acid were purchased from Sigma-Aldrich in this study.

Dual-LUC Assay

Dual-LUC assays were fulfilled using methods reported previously (Xiang et al., 2019). The promoter sequences of AaCER1 (MF144191), AaCYP86A1 (MF144190), ALDH1 (KC118525.1) and AaMYC2 (Figure S3) were cloned and inserted into pGreenII 0800-LUC plasmid to generate pCER1:LUC, pCYP86A1:LUC, pALDH1:LUC and pMYC2:LUC constructs as reporter vectors, respectively. Subsequently, these reporter vectors were transferred into A. tumefaciens strain GV3101 together with the pSoup plasmid. The AabZIP1 and AaMYC2 were inserted into the pHB plasmid driven by double CaMV 35S promoter as the effector vector and also transferred into A. tumefaciens strain GV3101. Meanwhile, the pHB-YFP (a yellow fluorescent protein construct driven by double 35S promoter) plasmid was transferred into GV3101 as a negative control. All engineering and control strains were inoculated into YEP liquid select medium and cultured overnight at 28. The agrobacterium cells were collected by centrifuge at 12000 rpm for 10 min and resuspended in the MS liquid to OD600 = 0.6 + 0.05. The acetosyringone (As, 100 mM, 1:500, v:v) and 2-(N-morpholino) ethanesulfonic acid (MES, 0.5M (pH=5.7), 1:50, v:v) were added to the resuspension and then were injected into tobacco leaves after being placed for 4 h at room temperature. Tobacco plants injected with agrobacterium cells were exposed to weak light for 48 h. A small piece of tobacco leaves (about 2 cm in diameter) was collected to 1.5 ml tube and immediately was ground in liquid nitrogen. The relative LUC/REN activity was tested using Dual-Luciferase(r) Reporter Assay System 10-Pack (Promega) according to the manufacturer's instructions.

Yeast one -hybrid assay

To investigate how AabZIP1 regulates the expression of AaCER1, AaCYP86A1 and AaMYC2, yeast one-

hybrid assays were fulfilled as described previously (Xiang et al., 2019). The AabZIP1 coding sequence was inserted into pB42AD plasmid containing the GAL4 activation domain (AD) through EcoRI and XhoI sites to generate pB42AD-AabZIP1 constructs as the prev. The 45 bp fragments containing one ABRE ciselement from AaCER1, AaCYP86A1 and AaMYC2 promoters, named pCER1-R1 (-987~-943), pCER1-R2 (-440~-396), pCER1-R3 (-147~-103), pCYP86A1-R1 (-1707~-1663), pCYP86A1-R2 (-1676~-1632), pMYC2-R1 (-1034~-1027), pMYC2-R2 (-998~-982), pMYC2-R3 (-678~-664) and pMYC2-R4 (-412~-393), were inserted into pLacZ plasmids through KpnI and XhoI sites as the bait, respectively. The pB42AD-AabZIP1 plasmid was co-transformed into yeast strain EGY48 with the above bait constructs, respectively. Similarly, the 45 bp fragments containing one G-box element from ALDH1 promoter, pALDH1-G1 (-987~-943) and pALDH1-G2 (-440~-396), were inserted into pLacZ plasmids as the bait, respectively. The pB42AD-AaMYC2 plasmid was co-transformed into yeast strain EGY48 with the above bait constructs, respectively. The yeast cells were grown on SD-Ura-Trp selective medium for 48 h at 30. All independent yeast cells were shifted into SD-Ura-Trp liquid medium and cultured overnight at 30, and then these cells were collected by microcentrifugation and resuspended in 100 μ l sterile water. Resuspended cells were grown on SD-Ura-Trp medium with 5bromo-4-chloro-3-indolyl-b-D-galactopyranoside (X-gal) for 24-48 h at 30. The empty pB42AD and pLacZ plasmids were used as negative controls. Five independent biological replicates were implemented for each experiment in this study. All sequences are listed in Table S2.

Electrophoretic mobility shift assay

The AabZIP1 and AaMYC2 were inserted into pEGX-6P-1 plasmid through EcoRI and XhoI sites to generate AabZIP1- and AaMYC2-pEGX-6P1 constructs respectively, and then transformed into *E. coli* strain BL21 (DE3) for expression to obtain recombinant protein. The expression of fusion proteins was induced in DE3 cells by adding 0.5 mM IPTG into LB liquid medium for 16 h at 18. Subsequently, the DE3 cells were collected by centrifuge and disrupted. The supernatant was filtered to purify the AabZIP1- and AaMYC2-GST proteins using BeyoGold GST-tag Purification Resin (Beyotime Biotechnology, China). The biotin-labeled 45 bp fragments containing ABRE*cis* -element from promoters of AaCER1, AaCYP86A1 and AaMYC2respectively, and fragments containing G-box element from ALDH1 promoter, were synthesized as the probe by Invitrogen (Guangzhou, China). Two single-stranded DNA fragments were incubated for 5 min at 98. Subsequently were -0.1 per cycle from 98 to 25, and then for 3 min at 25 to obtain an annealing product. EMSA was performed using the LightShift Chemiluminescent EMSA Kit (Pierce, Rockford, IL, USA) according to the manufacturer's instructions. The GST protein was used as the negative control. All probe sequences are listed in Table S3.

Results

Drought stress and ABA treatment induced the expression of AabZIP1 and wax biosynthesis genes

AabZIP1 plays an important role in ABA signaling, and its expression can be induced by both ABA and drought treatment (Zhang et al., 2015). To investigate the role of AabZIP1 in drought and ABA response in A .annua, wild type A. annua plants were subjected to drought stress and ABA treatment. qPCR analysis showed that AabZIP1 expression was significantly upregulated under drought stress and ABA treatment (Figure 1a, d). The expression level of AabZIP1 reached the highest at 3-6h after drought stress or ABA treatment, and then began to decline. This result was consistent with the previous report (Zhang et al., 2015), further demonstrating that AabZIP1 is involved in drought and ABA response in A .annua.

Cuticular wax acts as a protective barrier to prevent excessive water loss across the primary surface under water deficiciency. Many studies have shown that the expression of genes involved in wax biosynthesis is significantly increased under drought stress (Aharoni et al., 2004; Seo et al., 2011). So we detected the expression levels of wax-related biosynthesis genes under drought stress and ABA treatment. qPCR result showed that two wax biosynthesis genes, AaCER1 and AaCYP86A1, were markedly induced under drought stress and ABA treatment, and the highest expression levels of AaCER1 and AaCYP86A1 were detected at 6h or 12h after drought stress and ABA treatment (Figure 1b, c, Figure 1e, f). Taken together, these results

suggested that drought stress and ABA treatment induced the expression of AabZIP1 and wax biosynthesis genes.

Overexpression of AabZIP1 enhances tolerance to drought stress and cuticle wax accumulation in A. annua

To further explore the function of AabZIP1 in drought response in A. annua, the recombinant vector of pHB-AabZIP1 was constructed and transformed into A. annua to overexpress AabZIP1 as described previously (Shen et al., 2012). gRT-PCR analysis showed the transcription level of AabZIP1 was dramatically enhanced in AabZIP1-overexpression (OE-AabZIP1) transgenic A. annua plants by 9.05-15.64 times, compared to that in wild-type (Figure 2c). The expression levels of AaCER1 and AaCYP86A1, two wax biosynthesis genes, were significantly increased in all the three OE-AabZIP1 lines. Compared with the control, the expression levels of AaCER1 and AaCYP86A1 in OE-AabZIP1 plants increased by about 9.3-12.4 times and 2.5-4.0 times, respectively (Figure 2c). To investigate the drought resistance of OE-AabZIP1 A. annua plants, the OE-AabZIP1 and wild-typeA. annua plants were grown for 6 weeks in pots, and then subjected to drought stress. As shown in Figure 2a, the OE-AabZIP1 plants are more resistant to drought stress compared with the wild-type. After 2 days of drought stress, wild-type A. annua leaves exhibited slight wilting, while the leaves of the OE-AabZIP1 A .annua maintained flourishing. After 4 days of drought stress, wild-type leaves exhibited moderately wilting, while the leaves of OE-bZIP1 plants remained flourishing. After 6 and 8 days, wild-type plants severely withered, while OE-AabZIP1 plants were only moderately withered. After 4 days of water recovery, the OE-AabZIP1 plants recovered to normal condition as expected, while the wild-type plants died from severe water deficiency.

Cuticular wax accumulation is one of the important strategies to prevent excessive water loss and resist drought stress in plants. So the morphology of cuticular waxes crystals on the OE-AabZIP1 transgenic and wild-type A. annua leaves was detected by scanning electron microscopy (SEM). As shown in Figure 2b, abnormal wax deposition was observed in OE-AabZIP1 leaves, compared with wild-type plants. Moreover, the contents of cuticular waxes in mature leaves of OE-AabZIP1 and wild-type plants were analyzed by GC-MS according to the previously described method (Shi et al., 2017). OE-AabZIP1 transgenic lines (OE-1, OE-2 and OE-5) produced wax compounds (eicosane, pentacosane and 1-octacosane) at significantly higher levels than wild-type plants. The eicosane product was 10.8-16.9 μ g/g FW, pentacosane product was 3.8-6.2 μ g/g FW, 1-octacosanol was 5.5-9.3 μ g/g FW in the three lines (Figure 2d; Figure S2). In other words, the total wax production of OE-AabZIP1 plants was increased by 45% in OE1, 54% in OE2, and 66% in OE5, compared with that in wild-type plants, which is consistent with the SEM assays. The above results indicated that AabZIP1 positively regulates the accumulation of cuticular wax to enhance drought tolerance in *A. annua* leaves.

AabZIP1 enhances AaCER1 and AaCYP86A1 transcription by binding to their promoters

To further study how AabZIP1 regulates the expression of cuticular wax biosynthesis genes in A. annua leaves, dual-LUC assays were performed. When AabZIP1-YFP (green fluorescent protein) was expressed in N. benthamiana leaf cells harboring the pCER1:LUC or pCYP86A1:LUC plasmids, the promoter activities of AaCER1 and AaCYP86A1 were significantly increased compared with the negative YFP control. Among these reporter constructs, the LUC/REN value of pCER1:LUC and pCYP86A1:LUC were increased 7.4- and 2.1-fold than negative control (Figure 3a, b), respectively. The result indicated AabZIP1 can significantly enhance transcriptional activity of AaCER1 and AaCYP86A1 promoters in tobacco leaves.

It was previously reported that AabZIP1 can directly bind to ABRE *cis* -elements (ACGT-) in the target gene promoter (Zhang et al., 2015). Promoter analysis revealed that three and two ABRE *cis* -elements exist in *AaCER1* and *AaCYP86A1* promoters, respectively. Therefore, yeast one-hybrid (Y1H) assay was used to evaluate whether AabZIP1 can directly bind to these ABRE *cis* -elements. Y1H assay result indicated that AabZIP1 can directly bind to pCER1-R2 and pCYP86A1-R1 fragments (containing ABRE motif) in the *AaCER1* and *AaCYP86A1* promoters respectively. However, the pCER1-R1, pCER1-R3 and pCYP86A1-R2 fragments containing ABRE *cis* -element cannot be bound by AabZIP1 (Figure 3c, d). In addition,

the binding signal was weakened or disappeared in yeast EGY48 when the core sequences of the ABRE *cis* -elements in the pCER1-R2 and pCYP86A1-R1 fragments were mutated (Figure 3c, d).

Next, to further confirm the binding of AabZIP1 to ABRE-containing pCER1-R2 and pCYP86A1-R1 fragments, electrophoretic mobility shift assays (EMSAs) were conducted. The 45-bp length fragments containing ABRE *cis* -elements from pCER1-R2 and pCYP86A1-R1 were used as probes with biotin-labeled and unlabeled respectively. The GST-bZIP1 protein was induced in *E. coli* strain DE3 and GST protein was used as a negative control. Different amounts of unlabeled probes served as competitors to confirm the DNA binding specificity. Several group results indicated that AabZIP1 binds to the ABRE *cis* -elements of pCER1-R2 and pCYP86A1-R1 fragments from the *AaCER1* and *AaCYP86A1* promoters (Figure 3e, f). As the concentration of unlabeled probes increases $(1 \times, 10 \times, 100 \times)$, the phenomenon of AabZIP1 binding to labeled probes weakens or disappears in quantitative analysis (Figure 3e, f). Taken together, these results demonstrate that AabZIP1 enhances *AaCER1* and *AaCYP86A1* transcription by directly binding to their promoters.

AabZIP1 enhanced the transcription of DBR2 and ALDH1 by directly activating AaMYC2 expression

Many studies have indicated that TFs regulating artemisinin biosynthesis form a complex regulatory network (Chen et al., 2016; Xiang et al., 2019). It has been established that AabZIP1 directly enhances the transcription of ADS and CYP71AV1 by binding to ABRE cis -elements in their promoters. But it's not yet clear about the regulation of DBR2 and ALDH1 expression by AabZIP1. To address this issue, we detected the expression levels of *DBR2* and *ALDH1* in OE-AabZIP1 lines. qPCR result showed the expression levels of DBR2 and ALDH1 are significantly increased in OE-AabZIP1 lines, compared to that in wild type plants. Meanwhile, expression levels of ADS and CYP71AV1, as well as artemisinin and dihydroartemisinic acid contenes, are also significantly increased in OE-AabZIP1 lines (Figure 4a, b). Then, the effect of AabZIP1 on the transcriptional activity of DBR2 and ALDH1 promoters was further evaluated in tobacco leaves by dual-LUC assays. As expected, the transcriptional activity of DBR2 and ALDH1 promoters were enhanced by AabZIP1, and their activities are increased by 3.5 and 6.7-folds, respectively (Figure 4c, d). Promoter analysis showed there are two ABRE cis -elements in both DBR2 and ALDH1 promoters. Then the fragments containing these ABRE cis -elements were cloned separately, and inserted into pLacZ vectors respectively for Y1H assays. Unexpectedly, Y1H result showed AabZIP1 cannot directly bind to any of the ABRE *cis* -elements from *DBR2* and *ALDH1* promoters (Figure 4e, f). Based on these results, we infer that the regulatory mode in which AabZIP1 upregulates DBR2 and ALDH1 expression may be more complicated.

Then, we further analyzed the promoter sequences of previously reported TFs involved in artemisinin biosynthesis, and four ABRE*cis* -elements in AaMYC2 promoter were identified through promoter prediction software (Figure S3). So we are interested whether AabZIP1 regulates the transcription of AaMYC2. Dual-LUC assays were used to detect the effect of AabZIP1 on the transcriptional activity of AaMYC2 promoter in tobacco leaves. As expected, the transcriptional activity of AaMYC2 promoter was activated by AabZIP1, and its activity is increased by 3.7 folds compared with the control (Figure 5a, b). Y1H and EMSA results showed that AabZIP1 can directly bind to ABRE*cis* -elements in AaMYC2 promoter (Figure 5c, d). Besides, the expression level of AaMYC2 was upregulated 3.1-5.1 folds in OE-AabZIP1 transgenic plants compared to the wild type (Figure 5e). These results indicate that AabZIP1 directly activates the transcription of AaMYC2 by binding to its promoter.

In addition, it has been reported that AaMYC2 could directly activate the transcription of CYP71AV1 and DBR2 by binding to their promoters, thus promoting artemisinin biosynthesis; meanwhile, the expression of ALDH1 was also markedly increased in AaMYC2-overexpressing A. annua lines (Shen et al., 2016). But how ALDH1 expression is regulated by AaMYC2 is unclear. Here, dual-LUC analysis showed the transcriptional activity of ALDH1 promoter was enhanced by AaMYC2 (Figure 6a, b). Y1H and EMSA assays showed AaMYC2 can directly bind to the G-box motif of ALDH1 promoter (Figure 6c, d). These results indicate that AaMYC2 directly activates the transcription of ALDH1 by binding to its promoter. Taken together, the above results indicate that AabZIP1 could directly activate the transcription of AaMYC2 by binding to its promoter, thus enhancing the expression of artemisinin biosynthesis genes.

Discussion

AabZIP1 improves drought resistance of A. annua by promoting cuticular wax biosynthesis

Water deficiency is one of the main factors limiting plant growth and agricultural production. Plants have evolved a variety of regulatory mechanisms to effectively resist environmental stress. The accumulation of cuticular wax across the surface of plant organs is an important strategy for plants to prevent water loss and adapt to drought stress (Seo and Park, 2011). Many studies confirmed the expression of wax biosynthesis genes and cuticular wax content are increased markedly under water deficiency, in order to prevent water loss (Dimopoulos et al., 2020). Currently, the connection between drought stress and cuticular wax biosynthesis has been extensively investigated in multiple species (Seo et al., 2009; Pan et al., 2020). However, little attention has been paid t o the molecular link between drought stress and cuticular waxes biosynthesis in A. annua.

bZIP is one of the main transcription factor (TF) families related to abiotic stress (Wasilewska et al., 2008). bZIP A group plays an important role in ABA signaling transduction and response to abiotic stress (Kang et al., 2002; Que et al., 2015). AabZIP1, a bZIP A group TF from *A. annua*, was significantly induced by exogenous ABA treatment and drought stress (Zhang et al., 2015). However, it is not known whether AabZIP1 regulates wax biosynthesis in response to drought stress in *A. annua*.

To further explore the function of AabZIP1 in response to drought stress, we overexpressed the gene in A.annua and subjected the OE-AabZIP1 transgenic plants and wild type control to drought stress in this study. The phenotype analysis showed OE-AabZIP1 plants exhibited significantly stronger tolerance to water deficiency than wild type plants, indicating that AabZIP1 confers drought tolerance on A. annua plants (Figure 2a). Besides, we found overexpression of AabZIP1 in A. annua markedly improved the contents of eicosane, pentacosane and 1-octacosanol (Figure 2c, d), and OE-AabZIP1A. annua leaves are covered with abnormal wax deposition by SEM assays (Figure 2b). Therefore, we speculate AabZIP1 confers drought tolerance on A. annua plants by enhancing cuticle wax biosynthesis.

Furthermore, we found the expression of two wax biosynthesis genes, AaCER1 and AaCYP86A1, were upregulated under ABA and drought treatment, just as that of AabZIP1 (Figure 1). qRT-PCR results showed the OE-bZIP1 lines had significantly higher transcription levels of wax biosynthesis genes (AaCER1 and AaCYP86A1) than the wild type control (Figure 2c). So it is reasonable to infer that AabZIP1 positively regulates the expression of AaCER1 and AaCYP86A1. To investigate the mechanism how AaCER1 and AaCYP86A1 are regulated by AabZIP1, the promoter sequences of AaCER1 and AaCYP86A1 were isolated and analyzed, respectively. Two and three ABRE *cis* -elements were identified in the AaCER1 and AaCYP86A1 promoters respectively using prediction software. It was previously reported that bZIPs TF can directly bind to the ABRE *cis* -element in target promoters to activate their transcription (Yoshida et al., 2015, Zhang et al., 2015). Similarly, our results indicate that AabZIP1 activated the transcription of AaCER1 and AaCYP86A1 by directly binding to the ABRE *cis* -elements in their promoters according to dual-LUC, yeast one-hybrid and EMSA assays (Figure 3). In general, we demonstrate that AabZIP1 positively regulates cuticle wax biosynthesis by directly activating the expression of AaCER1 and AaCYP86A1, thus enhancing drought tolerance of A. annua (Figure 7).

AabZIP1 promotes artemisinin biosynthesis through diverse pathways

Artemisia annua is an important natural source of anti-malarial artemisinin, which plays an important role in protecting human health and global economic development. Unfortunately, the content of artemisinin in A. annua is extremely low and varies from 0.01% to 1% by dry weight, which is far from meeting the global demand. So it is quite important to elevate artemisinin biosynthesis in A. annua. Transcription factors (TFs) have irreplaceable advantages in regulating plant growth and metabolite biosynthesis, which can regulate the expression of multiple target genes in the metabolic pathway, thereby efficiently regulating the biosynthesis of specific metabolites. Up to now, a variety of transcription factors have been identified to positively regulate artemisinin biosynthesis. Among them, AabZIP1 has been identified to promote artemisinin biosynthesis through activating ADS and CYP71AV1 expression directly (Zhang et al., 2015), or indirectly via a AaGSW1dependent regulatory pathway (Chen et al., 2017). But there is still a lot to be explored about the roles of AabZIP1 in the regulatory network of artemisinin biosynthesis.

Here, we found that AabZIP1 can directly activate the transcription of AaMYC2 by binding to its promoter, and likewise, AaMYC2 can directly activate the transcription of ALDH1 by binding to its promoter (Figure 6). Besides, a former research has shown that AaMYC2 can directly activate the transcription of DBR2 and CYP71AV1 by binding to their promoters to increase artemisinin production (Shen et al., 2016). These results demonstrate that AabZIP1 positively regulates the transcription of DBR2 and ALDH1 through an indirect AaMYC2-dependent pathway, thus promoting artemisinin production (Figure 7). The above findings revealed to us that AabZIP1 could promote artemisinin biosynthesis by directly activating the expression of artemisinin biosynthesis genes (ADS and CYP71AV1), or via the mediation of other transcription factors, like AaGSW1 or AaMYC2.

Taken together, our study revealed the positive roles of AabZIP1 in regulating drought tolerance and artemisinin biosynthesis in A. annua, and expanded the knowledge for the regulatory network in artemisinin biosynthesis and response to environmental stress. Our results suggested AabZIP1 can be considered as a potential candidate gene for the development of A. annua plants with high artemisinin content and drought tolerance in metabolic engineering breeding.

Acknowledgements

This research was financially supported by the NSFC project (81973420 and 81803660), the National Key Research and Development Project (2019YFE0108700), the Natural Science Foundation of Chongqing (cstc2018jcyjAX0328) and the science funding of Sichuan Province (2020YJ0171).

Conflict of Interest Statement

The authors declare no conflict of interest.

References

Aharoni, A., Dixit, S., Jetter, R., Thoenes, E., Van, A. G., Pereira, A. (2004). The SHINE clade of AP2 domain transcription factors activates wax biosynthesis, alters cuticle properties, and confers drought tolerance when overexpressed in Arabidopsis. *The Plant Cell*, 16 (9), 2463-2480.

Anthony, J. R., Anthony, L. C., Nowroozi, F., Kwon, G., Newman., J. D., Keasling, J. D. (2009). Optimization of the mevalonate-based isoprenoid biosynthetic pathway in *Escherichia coli* for production of the antimalarial drug precursor amorpha-4,11-diene. *Metabolic Engineering*, 11 (1), 13-9.

Anjum, S. A., Wang, L. C., Farooq, M., Hussain, M., Xue, L. L., Zou, C. M. (2011). Brassinolide application improves the drought tolerance in maize through modulation of enzymatic antioxidants and leaf gas exchange. *Journal of Agronomy and Crop Science*, 197 (3), 177–185.

AbdElgawad, H., Avramova, V., Baggerman G., Van Raemdonck, G., ... Beemster, G. T. S. (2020). Starch biosynthesis contributes to the maintenance of photosynthesis and leaf growth under drought stress in maize. *Plant, Cell & Environment*, 43, 2254-2271.

Bernard, A., Domergue, F., Pascal, S., Jetter, R., Renne, C., Faure, J. D., Haslam, R. P., Napier, J. A., Lessire, R., Joubès, J. (2012). Reconstitution of plant alkane biosynthesis in yeast demonstrates that Arabidopsis ECERIFERUM1 and ECERIFERUM3 are core components of a very-long-chain alkane synthesis complex. *The Plant Cell*, 24 (7), 3106-3118.

Chen, M., Yan, T., Shen, Q., Lu, X., Pan, Q., Huang, Y., Tang, Y., Fu, X., Liu, M., Jiang, W., ... Tang, K. (2017). GLANDULAR TRICHOME-SPECIFIC WRKY 1 promotes artemisinin biosynthesis in *Artemisia* annua. New Phytologist, 214 (1), 304-316.

Dimopoulos, N., Tindjau, R., Wong, D. C. J., Matzat, T., Haslam, T., Song, C., Gambetta, G. A., Kunst, L., Castellarin, S. D. (2020). Drought stress modulates cuticular wax composition of the grape berry. *Journal*

of Experimental Botany, 71 (10), 3126-3141.

Graham, I. A., Besser, K., Blumer, S., ... Bowles D. (2010). The genetic map of *Artemisia annua* L. identifies loci affecting yield of the antimalarial drug artemisinin. *Science*, 327 (5963), 328-331.

Höfer, R., Briesen, I., Beck, M., Pinot, F., Schreiber, L., Franke, R. (2008). The Arabidopsis cytochrome P450 CYP86A1 encodes a fatty acid omega-hydroxylase involved in suberin monomer biosynthesis. *Journal of Experimental Botany*, 59 (9), 2347-2360.

Howell, S. H. (2013). Endoplasmic reticulum stress responses in plants. Annual Review of Plant Biology, 64, , 477-499.

Jung, K. H., Han, M. J., Lee, D. Y., Lee, Y. S., Schreiber, L., Franke, R., Faust, A., Yephremov, A., Saedler, H., Kim, Y. W., Hwang, I., An, G. (2006). Wax-deficient anther1 is involved in cuticle and wax production in rice anther walls and is required for pollen development. *The Plant Cell*, 18 (11), 3015-3032.

Kang, J. Y., Choi, H. I., Im, M. Y., Kim, S. Y. (2002). Arabidopsis basic leucine zipper proteins that mediate stress-responsive abscisic acid signaling. *The Plant Cell*, 14 (2), 343-357.

Kunst, L., Samuels, A. L. (2003). Biosynthesis and secretion of plant cuticular wax. *Progress in Lipid Research*, 42 (1), 51-80.

Livak, K. J., Schmittgen, T. D. (2001). Analysis of relative gene expression data using real-time quantitative PCR and the $2^{-\Delta\Delta^{\circ}T}$ method. *Methods*, 25, 402–408.

Lee, S. B., Suh, M. C. (2013). Recent advances in cuticular wax biosynthesis and its regulation in Arabidopsis. *Molecular Plant*, 6 (2), 246-249.

Lesk, C., Rowhani, P., Ramankutty, N. (2016). Influence of extreme weather disasters on global crop production. *Nature*, 529 (7584), 84-87.

Li, J., Casteels, T., Frogne, T., Ingvorsen, C., Honoré, C., Courtney, M., Huber, K. V. M., Schmitner, N., ... Kubicek, S. (2017). Artemisinins Target GABA_A Receptor Signaling and Impair α Cell Identity. *Cell*, 168 (1-2), 86-100.

Li, R. J., Li, L. M., Liu, X. L., Kim, J. C., Jenks, M. A., Lü, S. (2019). Diurnal Regulation of Plant Epidermal Wax Synthesis through Antagonistic Roles of the Transcription Factors SPL9 and DEWAX. *The Plant Cell*, *31* (11), 2711-2733.

Li, T., Sun, Y., Liu, T., Wu, H., An, P., Shui, Z., Wang, J., Zhu, Y., Li, C., Wang, Y., Jetter, R., Wang, Z. (2019). TaCER1-1A is involved in cuticular wax alkane biosynthesis in hexaploid wheat and responds to plant abiotic stresses. *Plant, Cell & Environment*, 42 (11), 3077-3091.

Miller, M. J., Walz, A. J., Zhu, H., Wu, C., Moraski, G., Möllmann, U., ... Boshoff, H. I. (2011). Design, synthesis, and study of a mycobactin-artemisinin conjugate that has selective and potent activity against tuberculosis and malaria. *Journal of the American Chemical Society*, 133 (7), 2076-9.

Obata, T., Fernie, A. R. (2012). The use of metabolomics to dissect plant responses to abiotic stresses. *Cellular and Molecular Life Sciences*, 69 (11), 3225-3243.

Pan, Z., Liu, M., Zhao, H., Tan, Z., Liang, K., Sun, Q., Gong, D., He, H., Zhou, W., Qiu, F. (2020). ZmSRL5 is involved in drought tolerance by maintaining cuticular wax structure in maize. *Journal of Integrative Plant Biology*, 00, 1-15

Que, F., Wang, G. L., Huang. Y., Xu, Z. S., Wang, F., Xiong, A. S. (2015). Genomic identification of group A bZIP transcription factors and their responses to abiotic stress in carrot. *Genetics and Molecular Research*, 14 (4), 13274-13288.

Seo, P. J., Xiang, F., Qiao, M., Park, J. Y, Lee, Y. N., Kim, S. G., Lee, Y. H., Park, W. J., Park, C. M. (2009). The MYB96 transcription factor mediates abscisic acid signaling during drought stress response in Arabidopsis. *Plant Physiology*, 151 (1), 275-289.

Seo, P. J., Park, C. M. (2011). Cuticular wax biosynthesis as a way of inducing drought resistance. *Plant Signaling & Behavior*, 6 (7), 1043-1045.

Shen, Q., Chen, Y. F., Wang, T., Wu, S. Y., Lu, X., Zhang, L., Zhang, F. Y., Jiang, W. M., Wang, G. F., Tang, K. X. (2012). Overexpression of the cytochrome P450 monooxygenase (cyp71av1) and cytochrome P450 reductase (cpr) genes increased artemisinin content in *Artemisia annua*(Asteraceae). *Genetics and Molecular Research*, 11 (3), 3298-3309.

Shen, Q., Lu, X., Yan, T., Fu, X., Lv, Z., Zhang, F., Pan, Q., Wang, G., Sun, X., Tang, K. (2016). The jasmonate-responsive AaMYC2 transcription factor positively regulates artemisinin biosynthesis in *Artemisia annua*. New Phytologist, 210 (4), 1269-1281.

Selvaraj, M. G., Ishizaki, T., Valencia, M., Ogawa, S., Dedicova, B., Ogata, T., Yoshiwara, K., ... Ishitani, M. (2017). Overexpression of an Arabidopsis thaliana galactinol synthase gene improves drought tolerance in transgenic rice and increased grain yield in the field. *Plant Biotechnology Journal*, 15 (11), 1465-1477.

Shi, P., Fu, X., Shen, Q., Liu, M., Pan, Q., Tang, Y., ... Tang, K. (2017). The roles of AaMIXTA1 in regulating the initiation of glandular trichomes and cuticle biosynthesis in *Artemisia annua*. New Phytologist, 217 (1), 261-276.

Tu Y. (2011). The discovery of artemisinin (qinghaosu) and gifts from Chinese medicine. *Nature Medicine*, 17 (10), 1217-1720.

Tran, K. Q., Tin, A. S., Firestone, G. L. (2014). Artemisinin triggers a G1 cell cycle arrest of human Ishikawa endometrial cancer cells and inhibits cyclin-dependent kinase-4 promoter activity and expression by disrupting nuclear factor-kB transcriptional signaling. *Anti-Cancer Drugs*, 25, 270–281.

Tabassum, T., Farooq, M., Ahmad, R., Zohaib, A., Wahid, A. (2017). Seed priming and transgenerational drought memory improves tolerance against salt stress in bread wheat. *Plant Physiology and Biochemistry*, 118, 362-369.

Vashisth, D., Kumar, R., Rastogi, S., Patel, V. K., Kalra, A., Gupta, M. M., Gupta, A. K., Shasany, A. K. (2018). Transcriptome changes induced by abiotic stresses in *Artemisia annua*. *Scientific Reports*, 8 (1), 3423.

Westfall, P. J., Pitera, D. J., Lenihan, J. R., Eng, D., Woolard, F. X., Regentin, R., Horning, T., Tsuruta, H., ... Paddon, C. J. (2012). Production of amorphadiene in yeast, and its conversion to dihydroartemisinic acid, precursor to the antimalarial agent artemisinin. *Proc Natl Acad Sci U S A*, 109 (3), 111-118.

Wasilewska, A., Vlad, F., Sirichandra, C., Redko, Y., Jammes, F., Valon, C., Frei dit Frey, N., Leung, J. (2008). An update on abscisic acid signaling in plants and more... *Molecular Plant*, 1 (2), 198-217.

Wang, W., Wang, Y., Zhang, Q., Qi, Y., Guo, D. (2009). Global characterization of Artemisia annua glandular trichome transcriptome using 454 pyrosequencing. BMC Genomics , 10 , 465.

Xiang, L., Jian, D., Zhang, F., Yang, C., Bai, G., Lan, X., Chen, M., Tang, K., Liao, Z. (2019). The coldinduced transcription factor bHLH112 promotes artemisinin biosynthesis indirectly via ERF1 in *Artemisia* annua. Journal of Experimental Botany, 70 (18), 4835-4848.

Xiong, C., Xie, Q., Yang, Q., Sun, P., Gao, S., Li, H., Zhang, J., Wang, T., Ye, Z., Yang, C. (2020). WOOLLY, interacting with MYB transcription factor MYB31, regulates cuticular wax biosynthesis by modulating CER6 expression in tomato. *The Plant Journal*, 103 (1), 323-337.

Yadav, R. K., Sangwan, R. S., Sabir, F., Srivastava, A. K., Sangwan, N. S. (2014). Effect of prolonged water stress on specialized secondary metabolites, peltate glandular trichomes, and pathway gene expression

in Artemisia annua L. Plant Physiology and Biochemistry ,74, 70-83.

Yoshida, T., Fujita, Y., Maruyama, K., Mogami, J., Todaka, D., Shinozaki, K., Yamaguchi-Shinozaki, K. (2015). Four Arabidopsis AREB/ABF transcription factors function predominantly in gene expression downstream of SnRK2 kinases in abscisic acid signalling in response to osmotic stress. *Plant, Cell & Environment*, 38 (1), 35-49.

Yan, T., Li, L., Xie, L., Chen, M., Shen, Q., Pan, Q., Fu, X., Shi, P., Tang, Y., Huang, H., Huang, Y., Huang, Y., Tang, K. (2018). A novel HD-ZIP IV/MIXTA complex promotes glandular trichome initiation and cuticle development in *Artemisia annua*. New Phytologist ,218 (2), 567-578.

Zhang, J. Y., Broeckling, C. D., Blancaflo, E. B., Sledge, M. K., Sumner, L. W., Wang, Z. Y. (2005). Overexpression of WXP1, a putative Medicago truncatula AP2 domain-containing transcription factor gene, increases cuticular wax accumulation and enhances drought tolerance in transgenic alfalfa (Medicago sativa). *The Plant Journal*, 42 (5), 689-707.

Zhang, F., Fu, X., Lv, Z., Lu, X., Shen, Q., Zhang, L., Zhu, M., Wang, G., Sun, X., Liao, Z., Tang, K. (2015). A basic leucine zipper transcription factor, AabZIP1, connects abscisic acid signaling with artemisinin biosynthesis in *Artemisia annua*. *Molecular Plant*, 8, 163-175.

Figure legends

Figure 1 Expression analysis of AabZIP1, AaCER1 and AaCYP86A1 in Artemisia annua plants under drought and abscisic acid (ABA) treatments. (a-c) Relative expression levels of AabZIP1, AaCER1 and AaCYP86A1 in plants subjected to drought for 0-24h. (d-f) Relative expression levels of AabZIP1, AaCER1 and AaCYP86A1 in plants under ABA treatment for 0-24h. Normal watering and 0.5% ethanol was used as mock in drought stress and ABA treatment, respectively. The data represents the means +- SD (n = 3). *P < 0.05, **P < 0.01 in student's t- test.

Figure 2 Analysis of drought resistance and cuticular wax of wild-type (WT) and overexpression of AabZIP1 (OE-AabZIP1)*Artemisia annua* plants. (a) Phenotypes of WT and OE-AabZIP1 plants before drought stress, after drought stress (2, 4, 6 and 8 days) and after water recovery while growing in soil, bars represent 10 cm. (b) SEM images of adaxial side leaves from WT and OE-AabZIP1 plants, the leaf surface of OE-AabZIP1 plants is covered with abnormal wax deposition, whereas WT plants surface is smooth and shows little wax deposition, bars represent 10 μ m. (c-d) Expression levels of *AabZIP1*, *AaCER1* and *AaCYP86A1* and contents of wax components. WT, wild-type; OE-AabZIP1-1, OE-AabZIP1-2 and OE-AabZIP1-5 are independent lines of AabZIP1-overexpressing *Artemisia annua*plants, The data represents the means \pm SD (n = 3), *P < 0.05, **P < 0.01 in student's t- test.

Figure 3 Biochemical assays between AabZIP1 and wax biosynthesis genes. (a) Diagrams of reporter and effector constructs in transient dual-luciferase assays (REN, renilla luciferase; LUC, firefly luciferase). (b) Effects of AabZIP1 on activities of the *AaCER1* and *AaCYP86A1* promoters in *N. benthamiana* cells. The YFP effector was used as a negative control, and the LUC/REN ratios of YFP were set as 1. The data represents the means \pm SD (n =3), **P < 0.01 in student's *t*- test. (c) Yeast one-hybrid assays between AabZIP1 and ABRE motifs of *AaCER1* promoter, blue plaques indicate protein-DNA interactions. (d) Yeast one-hybrid assays between AabZIP1 and ABRE motifs of *AaCER1* promoter. (f) EMSA assays between AabZIP1 and ABRE motifs of *AaCYP86A1* promoter. Unlabeled ABRE motifs were used as the competitor DNA at molar ratios of 1×; 50× and 100×.

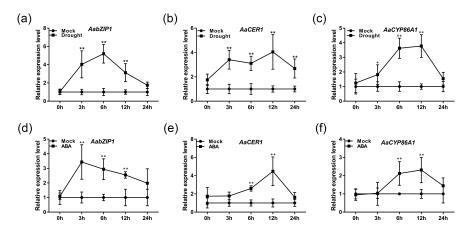
Figure 4Molecular analysis and detection of metabolites in wild-type and AabZIP1-overexpression Artemisia annua plants. (a) Expression levels of ADS, CYP71AV1, DBR2, and ALDH1. (b) Contents of artemisinin and dihydroartemisinic acid contents. WT, wild-type; OE-AabZIP1-1, OE-AabZIP1-2 and OE-AabZIP1-5 are independent lines of AabZIP1-overexpressing plants, the data represents the means \pm SD (n = 3), **P < 0.01 in student's t- test. (c) Diagrams of reporter and effector constructs in transient dual-luciferase assays (REN, renilla luciferase; LUC, firefly luciferase). (d) Effects of AabZIP1 on activities of the DBR2

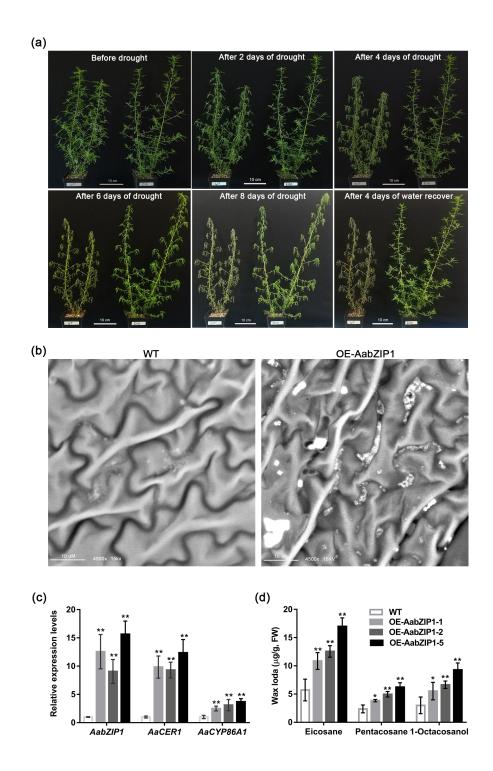
and ALDH1 promoters in *N. benthamiana* cells. The YFP effector was used as a negative control, and the LUC/REN ratios of YFP were set as 1. The data represents the means \pm SD (n = 3). (e) Yeast one-hybrid assays between AabZIP1 and ABRE motifs of *DBR2* promoter. (f) Yeast one-hybrid assays between AabZIP1 and ABRE motifs of *ALDH1* promoter.

Figure 5 Biochemical and molecular assays between AabZIP1 and AaMYC2. (a) Diagrams of reporter and effector constructs in transient dual-luciferase assays (REN, renilla luciferase; LUC, firefly luciferase). (b) Effects of AabZIP1 on activities of the AaMYC2 promoter in *N. benthamiana* cells. The YFP effector was used as a negative control, and the LUC/REN ratios of YFP were set as 1. The data represents the means \pm SD (n =3). (c) Yeast one-hybrid assays between AabZIP1 and ABRE motifs of *AaMYC2* promoter, blue plaques indicate protein-DNA interactions. (d) EMSA assays between AabZIP1 and ABRE motifs of *AaMYC2* promoter. Unlabeled ABRE motifs were used as the competitor DNA at molar ratios of 1×, 50× and 100×. (e) Expression levels of *AaMYC2 in* AabZIP1-overexpressing and wide-type*Artemisia annua* plants. WT, wild-type; OE-AabZIP1-1, OE-AabZIP1-2 and OE-AabZIP1-5 are independent lines of AabZIP1-overexpressing*Artemisia annua* plants, the data represents the means \pm SD (n = 3), **P < 0.01 in student's *t*- test.

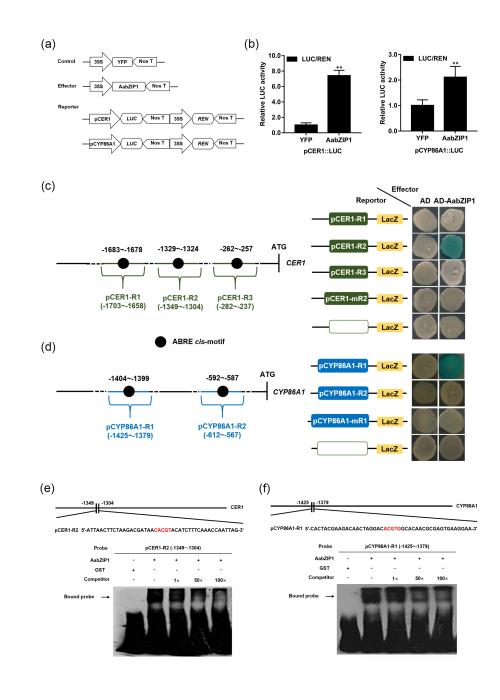
Figure 6 Biochemical assays between AaMYC2 and ALDH1. (a) Diagrams of reporter and effector constructs in transient dual-luciferase assays (REN, renilla luciferase; LUC, firefly luciferase). (b) Effects of AaMYC2 on activities of the ALDH1 promoter in N. benthamiana cells. The YFP effector was used as a negative control, and the LUC/REN ratios of YFP were set as 1, the data represents the means \pm SD (n =3), **P < 0.01 in student'st- test. (c) Yeast one-hybrid assays between AaMYC2 and G-box elements of ALDH1 promoter, blue plaques indicate protein-DNA interactions. (d) EMSA assays between AaMYC2 and G-box element of ALDH1 promoter. Unlabeled G-box element was used as the competitor DNA at molar ratios of 1×, 50× and 100×.

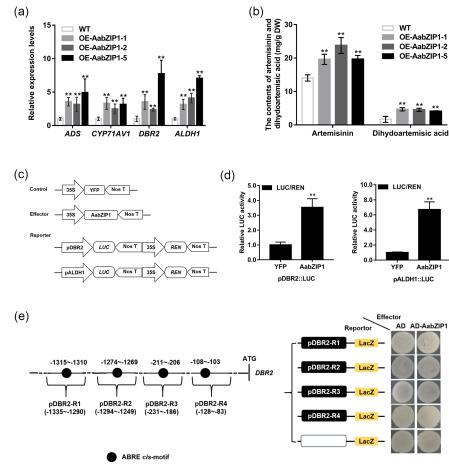
Figure 7 A simplified model illustrating that AabZIP1 enhances drought resistance by upregulating wax biosynthesis, and enhances artemisinin production by directly promoting the expression of AaMYC2, ADS and CYP71AV1 in A. annua plants.

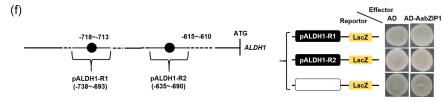


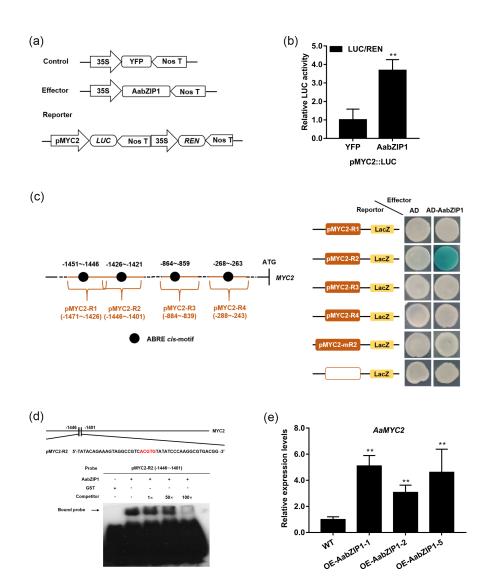


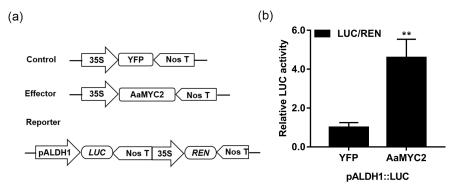
rel
e pre
ĕ,
ay
ma
tta
ñ
÷
ewe
riev
revi
E.
pe
en]
90
t l
no
nas
q p
'n
÷.
rint
prep
8
This
F
4
35
1879
618
16.
3411
8
64
-T
B
41
225.
_
Ę
org/
12
///qc
tps
ht
d.
sion.
issic
missic
missic
permissic
hout permissic
ithout permissic
without permissic
use without permissic
ithout permissic
o reuse without permissic
No reuse without permissic
ved. No reuse without permissic
ved. No reuse without permissic
reserved. No reuse without permissic
its reserved. No reuse without permissio
ghts reserved. No reuse without permissic
rights reserved. No reuse without permissic
rights reserved. No reuse without permissic
l rights reserved. No reuse without permissic
der. All rights reserved. No reuse without permissio
. All rights reserved. No reuse without permissio
inder. All rights reserved. No reuse without permissio
/funder. All rights reserved. No reuse without permissio
/funder. All rights reserved. No reuse without permissio
author/funder. All rights reserved. No reuse without permission
the author/funder. All rights reserved. No reuse without permission
is the author/funder. All rights reserved. No reuse without permission
the author/funder. All rights reserved. No reuse without permission
is the author/funder. All rights reserved. No reuse without permission
t holder is the author/funder. All rights reserved. No reuse without permissio
ght holder is the author/funder. All rights reserved. No reuse without permissic
yright holder is the author/funder. All rights reserved. No reuse without permissic
ght holder is the author/funder. All rights reserved. No reuse without permissic
copyright holder is the author/funder. All rights reserved. No reuse without permissic
copyright holder is the author/funder. All rights reserved. No reuse without permissic
The copyright holder is the author/funder. All rights reserved. No reuse without permissic
- The copyright holder is the author/funder. All rights reserved. No reuse without permission
22 - The copyright holder is the author/funder. All rights reserved. No reuse without permission
2022 - The copyright holder is the author/funder. All rights reserved. No reuse without permissic
far 2022 — The copyright holder is the author/funder. All rights reserved. No reuse without permissic
2022 - The copyright holder is the author/funder. All rights reserved. No reuse without permissic
30 Mar 2022 — The copyright holder is the author/funder. All rights reserved. No reuse without permissic
far 2022 — The copyright holder is the author/funder. All rights reserved. No reuse without permissic
30 Mar 2022 — The copyright holder is the author/funder. All rights reserved. No reuse without permissic
30 Mar 2022 — The copyright holder is the author/funder. All rights reserved. No reuse without permissic
Authorea 30 Mar 2022 — The copyright holder is the author/funder. All rights reserved. No reuse without permissic
30 Mar 2022 — The copyright holder is the author/funder. All rights reserved. No reuse without permissic
Authorea 30 Mar 2022 — The copyright holder is the author/funder. All rights reserved. No reuse without permissic

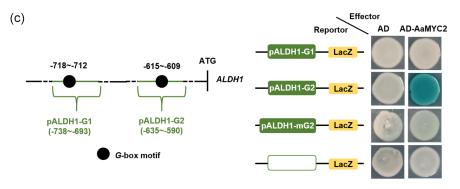












(d)

 -635	-590	ALDH1
		ALDIT

pALDH1-G2 5'-ATGTACGTTTTTGGTTCTATCACGTAACCAAACTGAACTAAAGAC-3'

Probe	pALDH1-G2 (-635~-590)				
AaMYC2		+	+	+	+
GST	+	-	-	-	-
Competitor		-	1×	50 ×	100×
Bound probe \longrightarrow			-		0

